Molecular Systems Biology 5; Article number 298; doi:10.1038/msb.2009.59
Citation: *Molecular Systems Biology* 5:298

www.molecularsystemsbiology.com

molecular systems biology

A mechanical bottleneck explains the variation in cup growth during FcγR phagocytosis

Jeroen S van Zon[1,4], George Tzircotis[1,2,4], Emmanuelle Caron[1,2] and Martin Howard[3,*]

[1] Centre for Integrative Systems Biology Imperial College (CISBIC), South Kensington Campus, Imperial College London, London, UK, [2] Centre for Molecular Microbiology and Infection, South Kensington Campus, Imperial College London, London, UK and [3] Department of Computational and Systems Biology, John Innes Centre, Norwich, UK
[4] These authors contributed equally to this work
* Corresponding author. M Howard, Department of Computational and Systems Biology, John Innes Centre, Norwich NR4 7UH, UK. Tel.: +44 1603 450 892; Fax: +44 1603 450 021; E-mail: martin.howard@bbsrc.ac.uk
Received 2.3.09; accepted 15.7.09

Phagocytosis is the process by which cells internalize particulate material, and is of central importance to immunity, homeostasis and development. Here, we study the internalization of immunoglobulin G-coated particles in cells transfected with Fcγ receptors (FcγRs) through the formation of an enveloping phagocytic cup. Using confocal microscopy, we precisely track the location of fluorescently tagged FcγRs during cup growth. Surprisingly, we found that phagocytic cups growing around identical spherical particles showed great variability even within a single cell and exhibited two eventual fates: a cup either stalled before forming a half-cup or it proceeded until the particle was fully enveloped. We explain these observations in terms of a mechanical bottleneck using a simple mathematical model of the overall process of cup growth. The model predicts that reducing F-actin concentration levels, and hence the deforming force, does not necessarily lead to stalled cups, a prediction we verify experimentally. Our analysis gives a coherent explanation for the importance of geometry in phagocytic uptake and provides a unifying framework for integrating the key processes, both biochemical and mechanical, occurring during cup growth.
Molecular Systems Biology **5:** 298; published online 18 August 2009; doi:10.1038/msb.2009.59
Subject Categories: membranes and transport; cell and tissue architecture
Keywords: F-actin; FcγR; mechanical bottleneck; membrane deformation; phagocytosis

Introduction

Phagocytosis is the process by which eukaryotic cells bind and engulf particulate material above 300 nm in diameter. Central to development, homeostasis and immunity, this basic cellular function is evolutionarily conserved from amoebae to mammals and is displayed by a large variety of cell types in metazoa (Stuart and Ezekowitz, 2008). Although the process of phagocytosis is essentially invariant, the nature of the material internalized varies greatly: it includes inorganic particles, microorganisms, apoptotic and senescent cells. At a cellular level, phagocytic uptake is a multistep process involving particle binding, circumferential wrapping of the phagocytozing cell around the particle and internalization of the particle in a membrane-bound intracellular compartment, the phagosome. At a molecular level, ligands on particles engage the extracellular domains of phagocytic receptors; receptor signaling then triggers intracellular signaling pathways that control local actin polymerization, thereby generating the force required for cortical deformation. Local actin dynamics is a vital component of phagocytic uptake: drugs such as latrunculin or cytochalasins (Zigmond and Hirsch, 1972; Axline and Reaven, 1974) that block actin polymerization, allow particle binding but disrupt membrane deformation, as do signaling mutants of phagocytic receptors (Mitchell, 1994; Cougoule, 2006). In agreement with the large variety of targets recognized, dozens of cell surface receptors can mediate phagocytic uptake either alone or as combinations of receptors (Groves *et al*, 2008). Importantly, the mechanisms and pathways governing particle internalization strictly depend on the signaling properties of the phagocytic receptors, rather than on the cell type involved (Caron and Hall, 1998; Lowry *et al*, 1998). This explains why studies of phagocytosis can equally well use professional phagocytes (e.g. *Drosophila* hemocytes, mammalian macrophages) or fibroblasts ectopically expressing phagocytic receptors (Ezekowitz, 1991; Odin *et al*, 1991).

The best understood experimental model of phagocytosis is the internalization of Immunoglobulin G (IgG)-coated particles by Fcγ receptors (FcγRs) (Swanson and Hoppe, 2004). On

ligation of FcγR, the membrane of macrophages progressively grows around the particle in a tight-fitted, zipper-like manner. Uptake depends on the establishment of IgG–FcγR interactions all around the particle, as shown using particles only half-coated with IgG (Griffin *et al*, 1976). The current hypothesis, supported by biochemical and mutagenesis data, suggests that ligand binding leads to the phosphorylation of two tyrosine residues in the cytoplasmic domains of FcγR, specifically in the immunoreceptor tyrosine activation motif (ITAM) region. Deletion of the whole cytoplasmic domain of FcγR, or substitution of these tyrosines for non-phosphorylatable amino acids (e.g. phenylalanines) reduces actin polymerization and disrupts particle uptake (Odin *et al*, 1991; Mitchell, 1994).

The zipper-like uptake is a localized process: for small enough particles, it involves only the segment of membrane bearing the receptors that initially interact with the particle and its immediate surroundings (Griffin and Silverstein, 1974). Moreover, for particles that are fully ingested, ratiometric imaging has shown that the dynamics of local F-actin accumulation and loss for each individual phagosome, although not synchronized, nevertheless follow the same pattern (Henry *et al*, 2004). One important consequence of these findings is that phagocytosis can be studied not only at the level of the whole cell, but also by considering each individual particle being phagocytosed as a discrete system. In our experimental and theoretical analysis, we therefore focused on phagocytosis at the level of individual particles.

Despite intensive experimental study, the overall process of phagocytic cup formation and, in particular, the interplay between receptor signaling and the mechanics of cortical deformation, remains poorly understood. These issues cannot be satisfactorily resolved by experiments alone, as the process of cup growth is intrinsically quantitative and relies on a subtle balance of pushing and restraining forces (Herant *et al*, 2006). Instead, we have used a unified experimental–theoretical approach to investigate the overall dynamics of cup growth. Experimentally, we examined the internalization of identical spherical particles coated with IgG in COS-7 cells transfected with wild-type (WT) FcγRs. We then carried out precise experiments tracking the location of FcγRs as a function of time during phagocytic cup growth. We found that phagocytic cups showed great variability even within a single cell and surprisingly manifested two eventual fates: a cup either stalled before forming a half-cup or it proceeded until the particle was fully enveloped. We explain these results using a simple mathematical model of the overall process of phagocytic cup growth. The model unifies the dynamics of receptor signaling/actin upregulation, together with the mechanics of membrane deformation, into a single framework. We then use the model to successfully predict the fate of cups associated with non-spherical particles (Champion and Mitragotri, 2006) and in cells in which actin polymerization has been compromised.

Results

Progression of phagocytic cup growth is highly variable even within a single cell

Using confocal microscopy we systematically studied the distribution of F-actin, using fluorescent phalloidin, and also WT FcγR tagged with green fluorescent protein (GFP) (see Materials and methods). First, we confirmed by phagocytosis assays that COS-7 cells expressing GFP-tagged WT FcγR properly ingested IgG-opsonized spherical latex particles 3 μm in diameter (Figure 1). As expected, cells left untransfected or transfected with GFP alone could not bind IgG-opsonized particles; neither could FcγR-transfected cells bind non-opsonized particles (data not shown). GFP-tagged, FcγR-transfected cells were presented with IgG-opsonized particles, fixed at 2-min intervals and imaged by confocal microscopy to obtain a complete picture of the cortical deformation as well as the distribution of FcγR and F-actin at various times following synchronizing cold treatment (see Materials and methods). Figure 2A shows typical examples of WT FcγR cup morphology at various time points. We find that for cells transfected with WT FcγR, phagocytic cups progress over the particle in a radially symmetric manner, leading to cup closure in 4–10 min for a significant fraction of particles. In addition, we find that F-actin and FcγR are strongly co-localized, as can be seen in Figure 2A and B, in agreement with previous observations (Greenberg *et al*, 1990; Caron and Hall, 1998).

However, we find great variability in the rate of cup progression from one particle to another, even within the same cell. This variability might partially reflect imperfect synchronization of phagocytosis in our experiments, but is likely to be an intrinsic property of phagocytic cup formation. To quantify the amount of variability in cup progression, we focus on a single parameter: the phagocytic cup size S, which measures the distance from the center of the phagocytic cup to its rim along the surface of the particle as defined by the distribution of the GFP-tagged FcγR (see Figure 2G). The cup size ranges from $S=0$, for the undeformed cell membrane, to $S=\pi R$, for a fully formed phagocytic cup, where R is the radius of the enveloped particle. In Figure 3A, we plot the distribution of cup sizes as a function of time for WT FcγR-transfected cells phagocytosing 3-μm diameter particles. We find that already at $t=0$ min, phagocytic cups show a wide distribution of cup sizes.

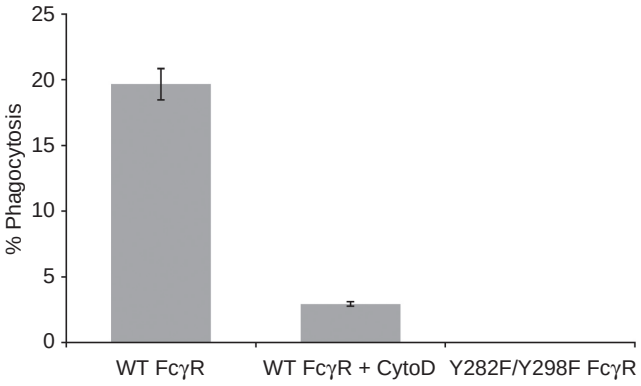

Figure 1 Phagocytosis assays in FcγR-transfected COS-7 cells. Cells were transfected with wild-type (WT) or Y282F/Y298F FcγR and subsequently challenged with IgG-opsonized particles for 10 min with or without 0.2 μM cytochalasin D. Fifty FcγR-expressing cells were scored for the number of particles attached but not internalized versus the number internalized. The fraction of successful internalizing events was then calculated.

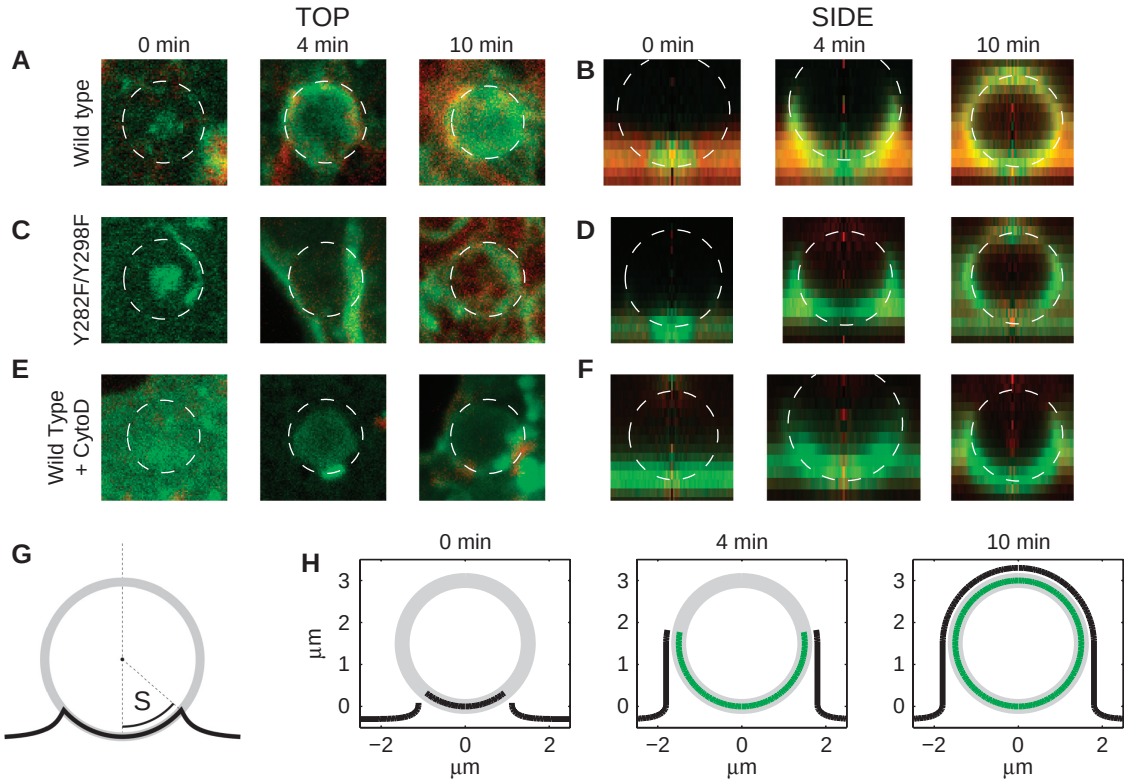

Figure 2 Typical cup shape and distribution of FcγR–GFP (green) and F-actin (red) in the phagocytic cup at 0, 4 and 10 min after the start of phagocytosis. COS-7 cells were transfected with (**A**, **B**) WT FcγR, (**C**, **D**) Y282F/Y298F FcγR, and (**E**, **F**) WT FcγR treated with 0.2 μM cytochalasin D. (A), (C) and (E) Representative images, showing the projection of fluorescence along the vertical axis. (B), (D) and (F) Corresponding averaged phagocytic cup cross-section (see Materials and methods for averaging methodology). For each image, the position of the particle is indicated by the dotted white lines. (**G**) Definition of the phagocytic cup size *S*, where *S* is the distance along the phagocytic cup from the cup center to the cup rim measured along the particle surface. (**H**) Shape and localization of FcγRs (green) as a function of time as predicted by our model for parameters corresponding to WT FcγRs.

The distribution of cup sizes becomes bimodal at later times

As phagocytosis progresses, the distribution of cup sizes remains broad but the average shifts to higher values. Surprisingly, we find that at later times the distribution of cup sizes becomes bimodal, with a broad distribution of cup sizes around $S=\pi R/2$, corresponding to half-cups, and a sharp peak that increases with time at $S=\pi R$, corresponding to fully enveloped particles. We observed very few cups between the half-cup and full-cup stage. This gap in the distribution between $S=\pi R/2$ and $S=\pi R$ probably reflects important features of the mechanics of cup formation, and underlines again that phagocytic cup growth, even of identical particles within a single cell, is extremely variable. Even for cups that do not progress past mid-cup, we find that their distribution shifts from a mean cup size of 1.5 μm at 0 min to 2.0 μm at 10 min. This finding is consistent with all cups growing in size as time passes, but with many being unable to grow past the half-cup position. Furthermore, we carried out experiments on the phagocytosis of 6-μm diameter particles, with very similar results: cups either stall at or before half-cup or else reach the full-cup stage (see Supplementary Figure S15).

Mathematical model

To understand the overall process of phagocytic cup growth, and, in particular, to explain the above observations, we have constructed a simple mathematical model of phagocytosis based on our experiments. The model combines (1) the diffusion of FcγRs on the curved geometry of the cell membrane, (2) their binding to ligands on the surface of the particle, (3) the subsequent upregulation of actin and (4) the resulting deformation of the cell cortex into a phagocytic cup.

To describe the FcγR-mediated signal transduction, we consider only the local concentrations of unbound, diffusing FcγRs; ligand-bound, immobile FcγRs; and F-actin. Importantly, our fluorescent recovery after photobleaching (FRAP) experiments (see Supplementary information) show that, in transfected COS-7 cells, FcγR delivery to the cup is primarily through diffusion rather than direct injection into the membrane from intracellular vesicles; hence we neglect the latter effect in our modeling. We also assume that free receptors bind ligands irreversibly (see Materials and methods), and that there is a maximum possible density of bound receptors on the particle. The bound receptors then stimulate local actin accumulation, which can also occur at a lower, basal rate.

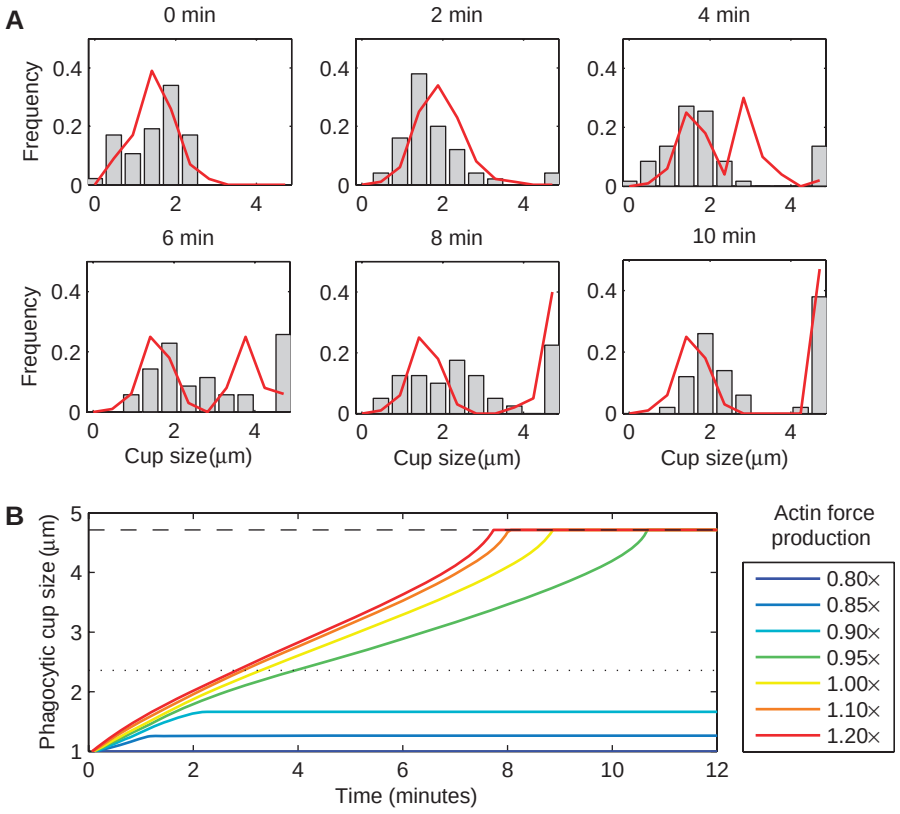

Figure 3 (**A**) Distribution of phagocytic cup sizes as a function of time for cells with WT FcγRs (gray bars, $n>35$ for all panels). A cup size of $S=\pi R\approx 4.7$ μm corresponds to a fully formed cup. Model simulations (red line), in which we plot the distribution of cup sizes for 100 particles with the force per unit of actin number used in Figure 2H multiplied by a factor drawn from a Gaussian distribution with mean 0.95 and s.d. 0.30. All other parameters take their WT values. (**B**) Phagocytic cup size as a function of time for solutions of our model in which the force per unit of actin number is multiplied by the specified factor. The cup size corresponding to a half-cup is indicated by a dotted line and that corresponding to a full cup by a dashed line.

Local F-actin accumulation then creates a mechanical force that leads to expansion of the phagocytic cup (Herant *et al*, 2006). The dynamics of cup size growth are described by a simple force–balance equation, with a pushing force (assumed to be proportional to the local F-actin concentration) and a restoring force due to the inherent stiffness of the cortex. To compute this restoring force, we first calculate the shape of the cup in the region away from the particle, assuming mechanical equilibrium. We can then find the total energy stored in the cup in both the bound and unbound regions as a function of the cup size S. Here we model the cell cortex and membrane in a unified manner as an elastic surface with a bending modulus κ and surface tension σ. These parameters depend on the local F-actin concentration, as regions of the membrane with a locally higher F-actin concentration will be stiffer. As the F-actin concentration is higher underneath the particle being phagocytosed in WT FcγR transfected cells due to receptor signaling, the bending modulus and surface tension will also be higher here than in other regions of the membrane. Once the energy of the membrane is known, it is then straightforward to calculate the restoring force. With this knowledge, we can numerically solve the model equations. Full details of our model and its implementation in terms of reaction–diffusion partial differential equations, a force–balance equation and an expression for the energy stored in an elastic membrane, can be found in the Materials and methods section and in the Supplementary information.

Shape of the phagocytic cup in the model agrees well with experiments

In Figure 2H, we show the shape of the cell membrane as well as the distribution of FcγRs, as obtained from our mathematical model (with WT parameters as described in the Materials and methods). For a given size of phagocytic cup, the shape of the membrane away from the particle is completely determined by the bending modulus κ and the surface tension σ. We find that using experimentally determined values for the parameters κ and σ, we can reproduce the different experimentally observed cup shapes within our model. In particular, our model predicts that even for moderate cup sizes (bigger than about a quarter of a fully formed cup) the unbound membrane drops away from the particle almost vertically (Figure 2H, middle panel), just as is seen in the experiments (Figure 2B, middle panel). In addition, the model naturally gives rise to the two different regimes of cortical deformation observed experimentally: an initial 'pedestal' regime for cups below the particles' widest point, $S<\pi R/2$, in which the particle rests on the cell, followed by a 'shell' regime for cups that have progressed past the widest point of the particle, at $S>\pi R/2$, in which the cell membrane doubles back on itself. In the shell regime, the profile of the membrane in regions not bound to the particle is, in our model, invariant.

A mechanical bottleneck in phagocytosis

In Figure 3B, we plot the phagocytic cup size as a function of time obtained from computer simulations of our mathematical model for 3-μm diameter particles. The rate of growth of the phagocytic cup size in our model is largely determined by the balance between the actin-generated force and the restoring force provided by the stiffness of the cell cortex. We consider $f(S)$, the force per unit length of cup circumference. In the shell regime $S>\pi R/2$, the deformation of the membrane not bound to the particle remains the same and for this reason, the restoring force per unit length of circumference is constant (see Materials and methods and the Supplementary information). For our parameters, $\tilde{f}_{\rm cup}=f_{\rm cup}(S>\pi R/2)\approx 155{\rm pN}\cdot\mu{\rm m}^{-1}$ and therefore the total force required to push out the cup at the widest point of the particle is about 1500 pN. Furthermore, our numerical results show that the restoring force $f_{\rm cup}$ for $S<\pi R/2$ is always smaller than its value $\tilde{f}$ during the second half of cup formation. This has important consequences for the mechanics of cup formation. Intuitively, we expect that there will be a maximum possible force per unit length that can be locally generated by polymerizing actin (see Supplementary information for a calculation of this maximum force in our model). If this maximum actin-generated force per unit length $f_{\rm actin}^{\rm max}<\tilde{f}_{\rm cup}$, phagocytosis will stall before it reaches the half-cup stage, $S=\pi R/2$. However, if $f_{\rm actin}^{\rm max}>\tilde{f}_{\rm cup}$, our model predicts that the phagocytic cup will always fully complete. In Figure 3B, we plot the cup size in our model as a function of time as we systematically change the force per unit of actin number, thereby directly altering $f_{\rm actin}^{\rm max}$. We indeed find that if we decrease this parameter by more than a factor of 0.95 from the value used in Figure 2H, phagocytic cups stall before they reach the half-cup stage. For higher values, however, phagocytosis progresses until the particle is fully enveloped. According to our model, therefore, if cups are able to pass the mechanical bottleneck at $S=\pi R/2$, they will always progress to the full-cup stage.

A mechanical bottleneck can explain the bimodal distribution of cup sizes

These two distinct behaviors as a function of the actin-generated force can explain the striking absence of phagocytic cups with a cup size between $S=\pi R/2$ and $S=\pi R$ at late time points, as observed experimentally in Figure 3A. We have carried out model simulations for 100 particles, in which the force per unit of actin number is drawn from a Gaussian distribution with mean 0.95 and s.d. 0.30, relative to the WT value used in Figure 2H. Such cup-to-cup variation reflects local differences within a single cell in the ability of the same levels of F-actin to generate force, potentially due to variation in the local activity of actin binding/cross-linking proteins. Moreover, we also impose a distribution of initial cup sizes (see Materials and methods), in agreement with the $t=0$ min data in Figure 3A. This initial variation may indicate that particles initially prefer to bind to pre-existing folds in the membrane in which, due to membrane curvature, there will be more receptors available for binding to the particle. In Figure 3A, we plot the resulting simulated distribution of cup sizes on top of the experimentally obtained distributions. We find that at later times, the simulated distribution separates itself into two peaks, similar to the experiments. In our model, we can identify the broad peak at $S<\pi R/2$ as corresponding to phagocytic cups stalled due to a lack of sufficient force generation, whereas the peak at $S=\pi R$ corresponds to particles that have a higher force production, sufficient for the cup to completely envelop the particle. Note that at intermediate times (especially at 4 min) the model predicts a peak between the half-cup and full-cup positions, a peak that is absent from the experimental data. This may indicate that, in our experiments, cups can traverse the distance between half- and full-cups more quickly than in our model. Despite this discrepancy, the eventual separation of the cup distribution in the model into two peaks is in good agreement with our experiments.

The above arguments hold in principle for variation in any of the parameters controlling cup growth, not just for variation in the force per unit of actin number. However, our procedure for opsonizing particles completely saturates the surface of the particle with ligands, making significant particle-to-particle variation in the maximum concentration of bound receptors improbable. Changes in the rates of F-actin accumulation are another possible source of cup size variation. However, changes in these parameters will be substantially masked by compensating changes in the stiffness of the cortex (see below). Hence, changes in the actin kinetics are less likely as a source of cup size variation. Local depletion of receptors can also lead to stalling of cup growth. However, in this case stalling occurs whenever FcγRs become locally depleted, which can happen at any given cup size rather than specifically at the half-cup stage. To confirm this, we have modified our model to allow for receptor depletion. We find that, depending on the total amount of FcγR available, stalling can occur at any point and, consequently, that receptor depletion cannot explain the almost complete absence of cups between the half-cup and full-cup stages in Figure 3A (see Supplementary information).

We have also carried out simulations for cup growth around 6-μm diameter particles. Importantly, all model parameters were fully specified by our 3-μm diameter particle experiments. Hence, our 6-μm particle experiments formed a rigorous test of the ability of the model to capture the full dynamics of phagocytosis in a new regime. Reassuringly, we found that our 6-μm particle simulations agreed very well with experiments with no changes in model parameters (see Supplementary Figure S15), although changes in the initial conditions were required and the timescale of cup formation was slightly slower in simulations than in the experiments. Once again, for the cup size distribution, we found a broad peak at half-cup together with a narrow peak corresponding to fully enveloped particles. This finding underlines our confidence in the model and in the presence of the mechanical bottleneck. Experiments on particles significantly smaller than 3 μm in diameter were hampered by resolution issues. Furthermore, we do not expect our model to quantitatively capture the phagocytosis of much larger particles, of the same order in size as the cell itself. To capture this scenario whole-cell modeling would be required.

The model predicts that phagocytic cup growth does not necessarily stall in cells with disrupted actin dynamics

A central feature of our model is that changes in the balance between the actin-generated and cortical restoring forces can lead to a marked alteration in the fate of phagocytic cups. Specifically, if the actin pushing force becomes smaller than the maximum restoring force, phagocytic cups will be unable to progress past the mechanical bottleneck. However, our model also predicts that simply reducing the actin accumulation rate could have potentially intricate consequences. This is because reducing the actin levels has two complementary effects: the maximum force that can be generated in the cup will be smaller, but because of reduced actin levels, the stiffness of the cortex will also be reduced, meaning that less force is needed to push the cup out. Whether a reduction in actin accumulation causes a cup to stall before completing, therefore, depends on the subtle ratio of these two effects. If the actin accumulation rates are reduced, but the elastic constants are reduced by a proportional amount, then a behavior similar to the WT will occur, with many cups being able to completely envelop the particle. However, if the actin accumulation rates are decreased by proportionally more than the elastic constants, then cups will stall before the halfway mark.

Model results are in good agreement with experiments in cells in which actin polymerization is reduced

To test whether the two different scenarios for cup growth detailed immediately above can be experimentally realized, we carried out experiments on cells in which actin polymerization is inhibited, either by mutation or drug treatment. We constructed GFP-tagged mutant receptors that either lack the entire cytoplasmic domain (Δ239 FcγR) or in which the two critical tyrosine residues within the ITAM domains have been replaced with phenylalanines (Y282F/Y298F FcγR), abrogating particle-induced actin polymerization at the cup rim (Odin *et al*, 1991; Mitchell, 1994). In addition, we also carried out experiments in which actin polymerization was blocked by treatment with cytochalasin D. Finally, we carried out a combined mutant/drug-treatment experiment, in cytochalasin-treated Y282F/Y298F FcγR-transfected cells.

First, in Figure 1, we compare the ability of cells transfected with WT and Y282F/Y298F FcγR, as well as cells with WT FcγR, treated with 0.2 μM cytochalasin D, to successfully attach to and internalize opsonized particles. As expected, we found that in all cases transfected cells are capable of binding particles, but that only cells expressing WT FcγR show significant levels of completed phagocytosis with internalization, confirming the central role of actin regulation in this process.

In Figure 2C, we show representative examples of cup morphology for different time points of cells transfected with Y282F/Y298F FcγR. We find that, in general, cup progression for both Y282F/Y298F and Δ239 FcγR mutants (data not shown) was not as radially symmetric as for WT FcγR. Instead, the rim of the cup sometimes showed irregular ruffles and projections. As expected, we also found that the co-localization between F-actin and FcγRs was much less pronounced than in WT cells. In general, the behavior of the Δ239 and Y282F/Y298F FcγR mutants was strikingly similar, confirming that the ITAM domain is the main regulator of phagocytic cup assembly within the receptor (data not shown). In Figure 4B, we show the distribution of cup sizes at 45 min for Y282F/Y298F FcγR cells. This distribution differs from the 45 min distribution for WT FcγR in Figure 4A in two aspects: in Figure 4B, we observe fewer fully grown cups and less of a pronounced gap between the half-cup and the full-cup stages. Nevertheless, we find in this case that fully grown cups can still be formed. To mathematically model Y282F/Y298F FcγR cells, we set the FcγR-stimulated F-actin accumulation rate to zero, whereas basal accumulation still occurs at the normal rate. As a consequence, both the F-actin concentration as well

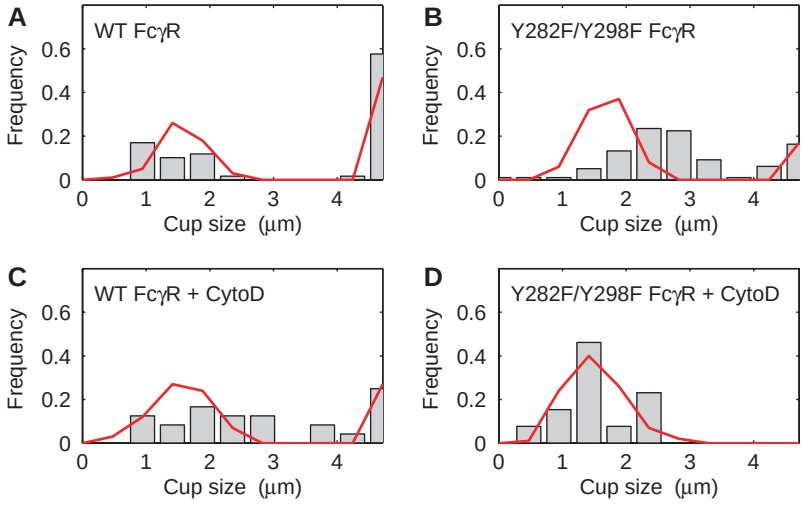

Figure 4 Distribution of phagocytic cup sizes at 45 min for (**A**) WT (n=59), (**B**) Y282F/Y298F FcγR (n=98), (**C**) WT FcγR treated with 0.2 μM cytochalasin D (n=24) and (**D**) Y282F/Y298F FcγR treated with 0.2 μM cytochalasin D (n=13). For cup size distributions at additional time points, see Supplementary information. Red lines show steady-state distributions as obtained by model simulations for 100 particles, as described in the text.

as σ and κ are unchanged away from the particle, but their values in regions bound to the particle are reduced to the same values as those in unbound regions. Fitting the remaining parameter values to the data (see Materials and methods), our model then produces results in qualitative agreement for the overall cup distribution (see Figure 4B, red line). Furthermore, our fitted model output is also qualitatively compatible with our experiments across the entire time series data set (see Supplementary Figure S12). Our results are, therefore, in accord with a scenario in which the actin-generated cup expansion force is reduced, but simultaneously the cup is less stiff and therefore easier to push out.

In Figure 2E, we show examples of cup morphology of WT FcγR-transfected cells treated with 0.2 μM cytochalasin D. As expected, we again found reduced co-localization of actin and FcγRs as compared with WT cells. Moreover, even though actin polymerization was suppressed globally within the cell, we still found a significant number of fully grown phagocytic cups, although formation required more time and there were fewer fully grown cups than in untreated WT FcγR transfected cells (see Figure 4C). To mathematically model cytochalasin D treated cells, we assume that F-actin accumulation is strongly suppressed but not entirely inhibited. We therefore reduce the basal and stimulated F-actin accumulation rates by factors of about 20 and 10, respectively. As a consequence, the cortex is mechanically weakened: we assume that both elastic constants are reduced everywhere from the values used in Figure 4A by a factor of 10. In principle, the effects of cytochalasin D may be more complex than assumed here. In particular, cytochalasin D may inhibit actin polymerization while leaving existing filaments and their cross-linking intact. This effect could be modeled by adjusting the bending modulus/surface tension parameters by different factors from the polymerization rates. However, much of the cortical cytoskeleton that is being deformed by cup growth is newly generated during phagocytosis and will, therefore, be of lower density and lesser stiffness in cytochalasin D-treated cells. For this reason, in our simulations of cytochalasin D-treated cells, we reduce the bending modulus/surface tension (which include the effects of cross-linking) by roughly the same factor as the reduction in actin polymerization rates. It should be noted that our results (here and below) are robust to changes in these reductions, provided the ratios of the accumulation rates to the elastic constants are maintained. Fitting the remaining parameters to the data (see Materials and methods), we find good agreement between the model (Figure 4C, red line) and experimental data, also across the entire time evolution of the cup (see Supplementary Figure S13).

However, when we treated Y282F/Y298F FcγR cells with 0.2 μM cytochalasin D, we found a markedly different distribution of cup sizes, with no cups observed past the half-cup stage even after 45 min (See Figure 4D). To mathematically model these cells, we set the stimulated actin accumulation rate to zero due to the lack of receptor signaling. Moreover, we reduce the basal rate by a factor of roughly 20 to mimic the effect of cytochalasin D. As a consequence of the much reduced actin levels, we assume that the elastic constants are reduced by a factor of 10 in regions not bound to the particle, with regions bound to the particle also having these same much reduced values. The remaining parameters were then fitted to the data (see Materials and methods). The agreement between the model (see Figure 4D, red line) and experiments is good, both at 45 min and at an earlier time (see Supplementary Figure S14). In this case, our results are entirely consistent with the actin-polymerizing forces being weakened to such an extent (by both a signaling deficiency and drug treatment) that there is insufficient force to advance the cup past the half-way mark, even though the cup is mechanically less stiff due to lesser actin accumulation.

In summary, our model predicts that reducing actin levels has a subtle effect, depending critically on whether a reduced actin pushing force is able to overcome a reduced cortical restoring force. This general prediction is amply verified in our experiments. When we move beyond this qualitative prediction to actually fitting our model to the experimental data, we again find an encouraging level of agreement in all cases.

Finally, we note that, despite the ability of Y282F/Y298F FcγR cells and WT FcγR cells treated with cytochalasin D to sometimes show what look like fully formed cups, the phagocytosis assay in Figure 1 shows that these mutants allow no particle ingestion. This indicates that formation of a full cup does not ensure successful particle internalization and that signaling from WT FcγR is required to ingest the particle after the cup has fully formed.

The model predicts a profound influence of particle geometry on phagocytic spread

It has previously been shown that the geometry of the particle being phagocytosed is as important for successful phagocytosis as the particle volume (Champion and Mitragotri, 2006). Macrophages challenged with elliptical disks completely phagocytosed such particles when presented with the highly curved end first, but stalled before reaching the half-way mark when presented with the flat side first. To address the impact of particle geometry on phagocytosis, we have used our model to study the uptake of spheroid particles. Spheroids with axes of lengths a and b are spheres that are squashed ($a > b$, oblate) or stretched ($b > a$, prolate) along the vertical axis.

In Figure 5, we systematically explore the extent of cup growth for spheroid particles with different axis lengths, a and b, but with otherwise identical parameters to those used in Figure 2H (see also the Supplementary information for more details). In general, we find that phagocytosis of spheroid particles follows the same qualitative pattern as that seen in an earlier study (Champion and Mitragotri, 2006). Prolate particles, presented with the highly curved end first, are taken up almost completely, whereas oblate particles, presented with the flat face first, stall around the half-cup stage. In our model, this effect is purely mechanical: for the prolate particle, the phagocytic cup encounters an area with high curvature when the cup is close to fully enveloping the particle. Regions of high curvature require large forces to induce cortical deformation, as the restoring forces from the cell cortex are high. Hence, for prolate particles, the cup either fully envelops the particle or comes very close to doing so. Note that high curvature is also found at small cup sizes. However, the initial conditions found experimentally (see Figure 3A and

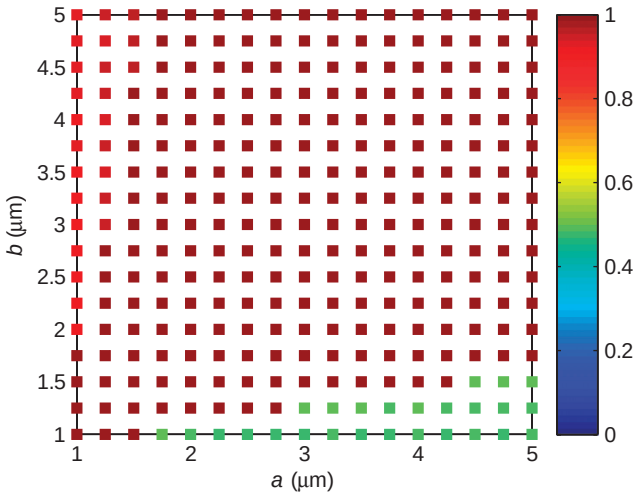

Figure 5 Phagocytosis of spheroid particles. Each point corresponds to a spheroid particle with axes of length *a* and *b*. The color indicates the extent of cup growth, in which 0.5 corresponds to cups stalled at the half-cup stage and 1 corresponds to fully completed cups.

Supplementary Figures S11–S13, S15) show that cups have already spread over this region even at the start of our experimental observations, possibly due to attachment to pre-existing membrane folds. For spherical particles (with constant curvature everywhere on the particle surface), our earlier results show that the maximum restoring forces occur from half-cup onwards, leading to a mechanical bottleneck at the half-cup stage. For oblate particles, this effect is accentuated. The region of higher curvature at the half-cup stage will cause even larger restoring forces in this region. The cup will, therefore, tend to stall at half-cup in an even more pronounced way than for spherical particles. This reasoning is confirmed in Figure 5.

Our model provides a rigorous testing ground in which to probe the effects of geometry on phagocytosis. Stalling of phagocytic cup growth is, according to our model, purely due to a failure to generate sufficient mechanical force to overcome the restoring force of the cell cortex. Within our model we can now compute where such stalling will occur, and indeed it often occurs close to where the restoring forces are highest, in regions of high particle curvature.

Discussion

Mathematical modeling is being used increasingly to improve our understanding of the complex interplay between biochemistry and physics in living organisms. Many biological processes are sufficiently complex that intuition alone cannot give reliable insights into the fundamental mechanisms at work; phagocytosis is an excellent example of such a complex system. The cellular uptake of inert particles, microorganisms and cells involves several hundreds of molecular regulators and effectors, according to high-throughput genomics and biochemical approaches (Morrissette, 1999; Garin, 2001; Stuart, 2007). Uptake is classically described as being composed of three stereotypical steps (particle recognition, actin-driven zipper-like spreading of the phagocytic membrane over the particle, and membrane fusion) (Groves *et al*, 2008; Swanson, 2008). Focusing on the second of these steps, and using a combination of imaging and mathematical modeling, we have been able to link the multifaceted elements underlying phagocytic spreading into a unified whole. Rather than attempting to reproduce the enormous complexity of the entire phagocytic cup signaling/membrane spreading system (a formidable task given the limitations of current knowledge), we instead attempted to construct a simplified model, based on our precise experimental observations of FcγR phagocytic cups. The successful encapsulation, in our model, of the overall mechanism of cup growth shows that a simple mathematical model can correctly explain key experimental results and point the way towards further critical experiments, even in an apparently complex biological system. Moreover, our model offers a conceptual framework in which the contribution of additional phagocytic regulators can be systematically investigated. As such, our model is a starting point for a detailed *in silico* model of phagocytosis that will greatly help in the quantitative dissection of this vital biological process.

Our model is based on experimental measurements of receptor diffusion and phagocytic cup progression in COS-7 cells expressing GFP–FcγR. Although COS-7 cells are fibroblasts and, therefore, not professional phagocytes, it is well established that fibroblasts have an intrinsic capacity for phagocytosis (Grinnell and Geiger, 1986). Nevertheless, it will still be important to repeat some of the experiments carried out here in macrophages or other professional phagocytes, to exclude an influence of cell size or FcγR overexpression on our observations. Moreover, our model as it currently stands does not incorporate membrane delivery. In macrophages, membrane has been shown to be delivered at sites of particle binding, although the nature of the donor compartment and mechanism(s) involved are still controversial (Touret, 2005). Despite these caveats, and because of the validity of the zipper model of phagocytosis for a wide variety of receptors (Lowry *et al*, 1998; Groves *et al*, 2008), we anticipate that our model and conclusions will apply to many other examples of zipper-like uptake, regardless of the types of receptors and phagocytic targets involved.

Interestingly, our data indicate a large variability in the size of individual phagocytic cups over the course of the experiments. This finding was unexpected, as it is generally assumed that centrifuging particles onto cells or challenging cells at 4°C, as we did, is sufficient to synchronize uptake. The variability is consistent with the idea of individual cups acting as discrete units that engage independently (Henry *et al*, 2004). In the absence of FcγR signaling at 4°C, such variation can be explained by the initial binding of particles to pre-existing membrane folds of varying size. However, after return to warm medium, we have shown, using our mathematical model, that the primary determinant of cup variability in phagocytosing cells is due to a mechanical bottleneck: some cups never generate sufficiently large deforming forces, and therefore stall where the restraining forces of the cell cortex are largest, at half-cup. The failure to generate sufficient force is not due to limiting receptor concentrations (Cannon and Swanson, 1992). More likely, it is due to limiting concentrations

(or availability of co-factors required for F-actin force generation, perhaps due to the large number of cups formed in our experiments. It is possible that expression of these co-factors will have to be upregulated in chronically challenged cells to permit a higher probability of cup closure. This issue calls for further investigation.

In cases in which the F-actin concentration levels, and hence the deforming forces, are reduced, our model predicts that cups do not necessarily stall. We have verified this prediction experimentally by tracking cup growth/FcγR concentrations in cells treated with an actin polymerization inhibitor and/or transfected with signaling-compromised mutant receptors. Our experimental results also underline that there is no strict correlation between receptor enrichment or actin polymerization at cups and cup completion, showing that receptor clustering or local actin polymerization are not, in themselves, good indicators of successful phagocytosis.

Our mathematical model also explains an important, previously unresolved issue, namely the influence of geometrical shape on the ability of particles to be taken up by phagocytosis (Champion and Mitragotri, 2006). Our model is able to give a coherent explanation for this effect: we find that the mechanics of cup deformation for oblate particles generally require higher maximal forces for cup growth than prolate particles. In the former case, receptors are still engaged and actin polymerizes locally, but insufficient force is generated for the membrane to extend beyond the particle equator; instead the cell membrane partially and locally spreads onto the particle. This scenario is consistent with the classical view of cell spreading as frustrated phagocytosis. Indeed, the mechanisms and signaling pathways controlling spreading and phagocytic uptake have often been compared (Cannon and Swanson, 1992; Cougoule *et al*, 2004). Our approach is able to give a rigorous underpinning to this analogy.

Materials and methods

Cells, plasmids and antibodies

COS-7 cells were obtained from American Type Culture Collection (ATCC) and cultured in Dulbecco's Modified Eagle's Medium (DMEM) supplemented with 10% fetal bovine serum (FBS) and penicillin/streptomycin (Invitrogen). cDNAs encoding WT and Y282F/Y298F human FcγRIIa from pRK5-FcγRIIa (Caron and Hall, 1998) and pRK5-Y282F/Y298F-FcγRIIa (Cougoule, 2006) were subcloned into pEGFP-N1 (Clontech) using primers 5′-ggtccaactgcacctcggt-3′ and 5′-ccccccgaattctgttattactgttgacatggtc-3′. The cytoplasmic tail truncation mutant, Δ239-FcγRIIa, was generated from the pRK5-FcγRIIa template using primers 5′-ggtccaactgcacctcggt-3′ and 5′-gggggggaattctcctgcagta gatcaaggccact-3′. Rabbit anti-bovine serum albumin (BSA) serum was purchased from Sigma-Aldrich. Alexa-conjugated secondary antibodies and phalloidin were purchased from Invitrogen.

Transfection and phagocytic challenge

COS-7 cells were transfected with GFP-tagged FcγRIIa constructs using an Amaxa Nucleofector and Nucleofector cell line kit R according to the manufacturers' instructions. For phagocytosis assays, transfected cells were seeded onto glass coverslips in 24-well plates at a density of 15 000 cells per coverslip and incubated at 37°C for 72 h. At 1 h before commencement of phagocytosis assays, cells were incubated for 1 h at 37°C with serum-free DMEM plus 10 mM HEPES (Invitrogen). Latex-polystyrene particles (Sigma-Aldrich) of 3 μm diameter or 6-μm diameter polybead(R) carboxylate modified polystyrene microspheres (Polysciences) were opsonized by first incubating overnight at 4°C with 3% BSA fraction V in PBS (Sigma-Aldrich) followed by incubation with 1:100 dilution of rabbit anti-BSA in PBS for 1 h at room temperature. Particles were re-suspended in ice-cold serum-free DMEM plus 10 mM HEPES at a concentration of 1.5×10^6 particles per ml and 500 μl of particle suspension was added to each coverslip. Plates were incubated on ice for 10 min to allow binding. Medium was then replaced with pre-warmed serum-free DMEM plus 10 mM HEPES and plates were floated on a 37°C waterbath, then processed for scoring or microscopy as described below. Experiments carried out on cells treated with cytochalasin D were carried out as above with an additional 20-min pre-incubation step with 0.2 μM cytochalasin D in serum-free DMEM plus 10 mM HEPES at 37°C immediately before the incubation of cells with opsonized particles. This concentration of cytochalasin D was included in all further incubation steps.

Scoring of phagocytosis

Plates were placed on ice after a 20-min incubation at 37°C and medium replaced with a 1:500 dilution of anti-rabbit Alexa 488 IgG in 3% BSA/PBS at 4°C for 5 min. Cells were then fixed with 4% paraformaldehyde/PBS, permeabilized and labeled with goat anti-rabbit Alexa 555 IgG in 3% BSA/PBS at room temperature for 30 min. For each transfection/treatment, 50 cells were scored for the number of particles that were internalized (labeled only with anti-rabbit Alexa 555 IgG) and those particles that were bound but not internalized (labeled with both anti-rabbit Alexa 555 IgG and anti-rabbit Alexa 488 IgG). The percentage efficiency of phagocytosis was then calculated as the average number of particles internalized divided by the average number of particles attached to or internalized by transfected COS-7 cells, multiplied by 100.

Imaging of phagocytic cups

Cells were fixed after incubation at 37°C for the appropriate amount of time with ice-cold 4% paraformaldehyde/PBS, permeabilized and labeled with goat anti-rabbit Alexa 633 IgG, and phalloidin Alexa 555 for visualizing F-actin. Z-series image stacks were acquired on a Zeiss LSM-510 confocal microscope using a step size of 0.4 μm.

Fluorescence recovery after photobleaching (FRAP)

COS-7 cells transfected with the WT FcγRIIa–GFP construct were seeded in glass-bottom 35 mm plates (MatTek) at a density of 60 000 cells per plate and incubated at 37°C for 72 h. An inverted Zeiss LSM-510 confocal microscope with a 37°C incubation chamber equilibrated at 5% CO_2 was used for imaging. For each cell, a region of interest corresponding to no more than 20% of the total cell area was selected and photobleached using a 30-mW Argon laser at full power for 3 s. Photobleaching recovery was followed at 1-s intervals for 90 s.

Phagocytic cup analysis

In the resulting confocal images, we manually selected all particles that were both fully in the field of view along the z-axis and not obscured by large fluorescent background structures, such as FcγR-containing vesicles or actin cables. The full three-dimensional image stacks of phagocytic cups were converted into the two-dimensional cross-sections shown in Figure 2B, D and F by averaging the fluorescence intensity around the z-axis through the center of the particle in the following way: for each height z and distance r to the z-axis, the resulting intensity in the cross-section was obtained by averaging the intensity in the full three-dimensional image stack over all pixels (x',y',z') with $x'^2+y'^2=r^2$ and $z'=z$. For each time point, we manually obtained the distribution of phagocytic cup sizes by measuring the progression of FcγR–GFP fluorescence along the surface of the particle. For each scenario (WT or Y282F/Y298F FcγR cells, treated or not treated with cytochalasin D) and time point, we obtained data for >35

phagocytic cups from >4 different cells. All image analyses were carried out in MATLAB (Mathworks).

Mathematical model equations

We assume the phagocytic cup is radially symmetric around the vertical axis of the particle. We, therefore, consider the local concentrations of unbound diffusing FcγRs, $p(s,t)$, ligand-bound immobile FcγRs, $P(s,t)$ and F-actin, $a(s,t)$, where s is the distance measured along the membrane from the cup center. This leads to the following (reaction–diffusion) equations for the dynamics of the signaling pathway:

$$\frac{\partial p(s,t)}{\partial t} = D\left[\frac{\partial^2}{\partial s^2} + \frac{1}{\mu(s)}\frac{d\mu(s)}{ds}\frac{\partial}{\partial s}\right]p(s,t) - k_a[P_0 - P(s,t)]p(s,t) \quad (1)$$

$$\frac{\partial P(s,t)}{\partial t} = k_a[P_0 - P(s,t)]p(s,t) \quad (2)$$

$$\frac{\partial a(s,t)}{\partial t} = k_p P(s,t) + k_{p,b} - k_{dp}a(s,t). \quad (3)$$

Here, D is the unbound FcγR diffusion constant and P_0 the maximum concentration of bound receptors (taken to be zero in regions not in contact with the particle). The effect of the local, curved geometry of the phagocytic cup on receptor diffusion is entirely taken into account by the term proportional to $\mu^{-1}\mathrm{d}\mu/\mathrm{d}s$, where $\mu(s)$ is the shortest distance from the membrane at s to the vertical axis through the center of the particle (see Supplementary information). Furthermore, we assume that free receptors bind ligands irreversibly (see below) with a reaction constant k_a. Bound receptors stimulate local actin accumulation at a rate k_p, whereas actin disassembly occurs at a rate k_{dp}. In addition, we assume that basal, FcγR-independent F-actin accumulation occurs at a lower rate, with a reaction constant $k_{p,b}$. Local F-actin accumulation then leads to mechanical deformation of the phagocytic cup. We describe the shape of the cup by a single parameter, the phagocytic cup size S(t). The entire dynamics of the phagocytic cup is described by the following equation:

$$\frac{dS(t)}{dt} = \gamma \max\left(0, \left[2\pi R f_0 \int_{S(t)-\lambda}^{S(t)} ds\, \sin(s/R)a(s,t)\right] + F_{\mathrm{cup}}(S(t))\right)P(S,t). \quad (4)$$

The first term on the right-hand side is the force due to actin polymerization, which we assume is proportional to the total amount of F-actin in a region of width λ around the entire rim of the cup, and where f_0 is the force generated per unit of actin number. We calculate the total amount of actin by integrating $a(s,t)$ over the surface of the particle between $s=S(t)-\lambda$ and $s=S(t)$. The second term, F_{cup}, is the restoring force on the cup rim due to the deformation of the cell cortex and is discussed further below. Owing to the small Reynolds number, we assume the dynamics of cup deformation is over-damped, in which it is the rate of increase of the cup size that depends linearly on the balance between the actin-generated force and the restoring force, with the parameter γ as the proportionality constant. The requirement that bound FcγR is present at the rim of the cup to provide the anchorage for further cup expansion (Griffin and Silverstein, 1974) leads to the dependence of equation (4) on $P(S,t)$. Finally, as we assume that receptor binding is irreversible, $S(t)$ can never decrease.

To calculate the restoring force, F_{cup}, in equation 4), we first need to calculate the shape and then the resulting total energy of the cup as a function of the cup size S. We model the cell cortex and membrane in a unified manner as an elastic surface with bending modulus κ and surface tension σ, in which case the total energy E is given by the energy functional: (Boal, 2002)

$$E = \int dA[2\kappa H^2 + \sigma]. \quad (5)$$

Here the integral is over the entire membrane area, H is the local mean curvature of the cell membrane and where κ and σ depend on the local actin concentration, and therefore, on position. We assume here that the contribution from the Gaussian curvature can be neglected (see Supplementary information). The energy stored by the membrane in contact with the particle is straightforward to calculate. However, as phagocytosis progresses the unbound membrane away from the particle is also increasingly deformed. We obtain an equation for the unbound membrane in mechanical equilibrium by writing down the full non-linear Euler–Lagrange equation that minimizes E. We subsequently find the shape of the unbound membrane as a function of S by numerically solving this equation with appropriate boundary conditions. Once the full shape of the cup is known, we can calculate the energy E for both the bound and unbound sections of membrane, as well as the geometric factor $\mu(s)$ in equation 1). Finally, the restoring force is given by $F_{\mathrm{cup}}(S) = -\mathrm{d}E(s)/\mathrm{d}s|_{s=S}$. Complete details of our model and its numerical integration can be found in the Supplementary information.

Mathematical model assumptions

Owing to the difficulty in obtaining quantitative data, we have simplified certain aspects of phagocytic cup growth in our model, in which we focus instead only on the key processes involved. A large network of signaling molecules is involved in the upregulation of actin polymerization (Swanson and Hoppe, 2004), which in our model is summarized as receptor binding directly stimulating actin accumulation. The modification of phospholipids (Swanson and Hoppe, 2004) and targeted membrane delivery (Hackam, 1998; Bajno, 2000; Niedergang *et al*, 2003) also have a well-documented function in macrophage phagocytosis. In our model, we neglect these processes, particularly as some lipid-modifying enzymes regulate phagocytosis primarily around larger particles (Swanson and Hoppe, 2004). Local membrane delivery also does not noticeably influence FcγR dynamics in transfected COS-7 cells (see Supplementary information). Myosin has not been incorporated in our model, as its reported function in cup formation is modest (Herant *et al*, 2006). Diffusion of transmembrane receptors, such as FcγR, is believed to be restricted in regions with a dense actin cytoskeleton (Andrews, 2008). As most FcγRs inside the cup rim, in which actin filaments are abundant, are bound and immobile, we use the same diffusion constant for unbound receptors everywhere on the membrane. We also assume that the rate of actin accumulation at the cup rim is independent of the restoring force on the rim. Our treatment of the actin dynamics is especially simple, as we assume its accumulation follows the simplest possible linear dynamics without incorporating any specific details of polymerization or depolymerization.

Furthermore, we assume that the binding of the FcγRs to their ligands (and the binding of IgG to the bead) is irreversible. This assumption is supported by *in vitro* measurements of receptor–ligand affinity for FcγR/IgG, in which a value of $10^7\,\mathrm{M}^{-1}$ was found, indicative of moderately strong binding (Gessner *et al*, 1998). The affinity of IgG for its ligand on the bead can also be estimated from the literature, and is again expected to be larger than about $10^7\,\mathrm{M}^{-1}$ (Phillips *et al*, 1987). Moreover, even if our assumption of irreversibility were relaxed, we would probably still see similar behavior; provided the majority of receptors within the particle–cell contact area are bound to ligands, the sheer number of bonds ensures that cup extension itself is essentially irreversible. It should be noted that we do not include the energy of receptor–ligand binding in our expression for E given above. This omission distinguishes our approach from, for example, models of receptor-mediated endoytosis (Gao *et al*, 2005) and follows from the exact way we envision cup expansion to occur: first, actin polymerization at the rim pushes out the cortex by a small fraction. This brings part of the membrane in contact with the surface of the particle, allowing subsequent binding of receptors to ligands on the particle. Force production is only required for the first stage. The receptor–ligand binding in the subsequent stage only functions as a holdfast to allow the cell to push against the particle for the next round of cup expansion. As the receptor–ligand interaction has no function during the first stage, we calculate the force required for the expansion by taking into account only the energy of mechanical deformation of the cortex.

Previous attempts to model FcγR-mediated phagocytosis have employed a finite element model of cytoskeletal flow (Herant *et al*, 2006). Our approach contrasts with and complements this model in several ways: first, our assumptions of mechanical equilibrium in the cell cortex and radial symmetry radically simplify our model, thereby exposing the core elements required for successful phagocytic cup growth. Furthermore, we explicitly model the diffusion of receptors along the curved cell membrane and allow the binding of these dynamic receptors to ligands to trigger actin accumulation. Finally, we present results that go well beyond those of the study by Herant *et al* (2006), in particular our analysis of the variability of cup progression, the existence of a mechanical bottleneck, our analysis of receptor mutants and cytochalasin D treated cells, and our treatment of cup formation for spheroid particles.

WT model parameters

Both the bending modulus κ and the surface tension σ have been measured experimentally in resting cells. Outside of the cup rim, we use $\kappa(s>S)=1\,\mathrm{pN\,\mu m}$ (Zhelev *et al*, 1994) and $\sigma(s>S)=25\,\mathrm{pN\,\mu m^{-1}}$ (Zhelev *et al*, 1994; Herant *et al*, 2005). For the parameters used in our simulations, we find that the actin concentration inside the cup rim is approximately constant throughout phagocytic cup growth. Hence, in our model κ and σ inside the cup rim are not taken to explicitly depend on the local actin concentration. Instead, we assume that the elevated actin concentration inside the cup rim increases the local stiffness by a factor of 5 so that $\kappa(s\leqslant S)=5\,\kappa(s>S)$ and $\sigma(s\leqslant S)=5\sigma(s>S)$. We have measured the receptor diffusion constant directly by FRAP (see Supplementary information) and use a value of $0.3\,\mathrm{\mu m^2\,s^{-1}}$. As we cannot measure the absolute concentration of FcγR and F-actin in our experiments, we set the initial FcγR concentration to $p_0=1\,\mathrm{\mu m^{-2}}$. All other parameters were fitted to match the timescale of phagocytosis as well as the experimentally observed distribution of actin and FcγRs (see Supplementary Figures S11–S14). Unless indicated otherwise, we use the following values: $R=1.5\,\mu$m, $P_0=10p_0$; $k_a=5\,\mathrm{\mu m^2\,s^{-1}}$; $k_p=3\,\mathrm{s^{-1}}$; $k_{p,b}=10\,\mathrm{\mu m^{-2}\,s^{-1}}$; $k_{dp}=10\,\mathrm{s^{-1}}$; $f_0=825$ pN per unit of actin number; $\lambda=0.05\,\mu$m; and $\gamma=1\times10^{-4}\,\mathrm{\mu m^3\,s^{-1}\,pN^{-1}}$. The rate k_a is chosen to be high enough that FcγRs diffuse only a short distance into the contact region between the membrane and the particle before binding. As FcγR signaling only leads to local force production, we choose λ to be small compared with the particle size. The reaction constants k_p, $k_{p,b}$ and k_{dp} are chosen so that the actin dynamics is fast on the timescale of phagocytosis. Finally, for simulations with variation in the initial cup size for particles of radius 1.5 μm, we use a Gaussian distribution with mean cup size $S(0)=1.5\,\mu$m and s.d. 0.5 μm, in agreement with data in Figure 3A and also Supplementary Figures S12 and S13; in other cases with 1.5-μm particles (Figures 2H, 3B and 5) we use a fixed initial condition of $S(0)=1\,\mu$m. For particles with radius 3 μm, we use an initial Gaussian distribution with mean cup size $S(0)=2.5\,\mu$m and s.d. 0.75 μm, in agreement with data in Supplementary Figure S15.

Parameters for Y282F/Y298F FcγR and/or cytochalasin D-treated cells

The complete parameter values for these scenarios are: for Y282F/Y298F FcγR cells: $k_p=0$; $\gamma=1\times10^{-6}\,\mathrm{\mu m^3\,s^{-1}\,pN^{-1}}$; $\sigma(s)=25\,\mathrm{pN\,\mu m^{-1}}$ and $\kappa(s)=1\,\mathrm{pN\,\mu m}$; for cytochalasin D-treated WT FcγR cells: $k_p=0.25\,\mathrm{s^{-1}}$; $k_{p,b}=0.55\,\mathrm{\mu m^{-2}\,s^{-1}}$; $\gamma=5\times10^{-7}\,\mathrm{\mu m^3\,s^{-1}\,pN^{-1}}$; $\sigma(s\leqslant S)=12.5\,\mathrm{pN\,\mu m^{-1}}$; $\sigma(s>S)=2.5\,\mathrm{pN\,\mu m^{-1}}$; $\kappa(s\leqslant S)=0.5\,\mathrm{pN\,\mu m}$ and $\kappa(s>S)=0.1\,\mathrm{pN\,\mu m}$; for cytochalasin D-treated Y282F/Y298F FcγR cells: $k_p=0$; $k_{p,b}=0.55\,\mathrm{\mu m^{-2}\,s^{-1}}$; $\gamma=1\times10^{-6}\,\mathrm{\mu m^3\,s^{-1}\,pN^{-1}}$; $\sigma(s)=2.5\,\mathrm{pN\,\mu m^{-1}}$ and $\kappa(s)=0.1\,\mathrm{pN\,\mu m}$. Parameters not listed above are unchanged from their WT values.

Model implementation

We discretized equations. 1–3) and integrated them numerically using an explicit Euler scheme with time step $\Delta t=2\times10^{-5}\,$s and lattice spacing $\Delta s=5\times10^{-3}\,\mu$m. We used a boundary condition $p(s)=p_0$ at $s=10\,\mu$m for 3-μm diameter particles and at $s=20\,\mu$m for 6-μm diameter particles. The updated F-actin concentration was then used in the equation 4), which was discretized and integrated numerically using the same time step Δt, to obtain the updated cup size. The updated shape of the unbound membrane was then obtained numerically using a shooting algorithm to solve the Euler–Lagrange equations that minimized equation 5). The resulting updated stored energy could then be calculated using equation 5), which, in turn, permitted the calculation of the restoring force through numerical differentiation. Finally, the densities were updated again as a result of changes to the cup shape. For more details, see Supplementary information.

Supplementary information

Supplementary information is available at the *Molecular Systems Biology* website (www.nature.com/msb).

Note added in proof

The authors would like to dedicate this manuscript to the memory of Dr Emmanuelle Caron, who passed away shortly after this work was completed. Emmanuelle was an exceptionally generous and talented scientist; she will be sorely missed by all who knew her.

Acknowledgements

We thank Richard Morris for a critical reading of the paper. This study was supported by financial support from the Biotechnology and Biological Sciences Research Council (BBSRC) through the Centre for Integrative Systems Biology at Imperial College (CISBIC), BB/C519670/1. MH acknowledges additional financial support from the Royal Society.

Conflict of interest

The authors declare that they have no conflict of interest.

References

Andrews NL, Lidke KA, Pfeiffer JR, Burns AR, Wilson BS, Oliver JM, Lidke DS (2008) Actin restricts FcεRI diffusion and facilitates antigen-induced receptor immobilization. *Nat Cell Biol* **10:** 955–963

Axline SG, Reaven EP (1974) Inhibition of phagocytosis and plasma membrane mobility of the cultivated macrophage by cytochalasin B. Role of subplasmalemmal microfilaments. *J Cell Biol* **62:** 647–659

Bajno L, Peng XR, Schreiber AD, Moore HP, Trimble WS, Grinstein S (2000) Focal exocytosis of VAMP3-containing vesicles at sites of phagosome formation. *J Cell Biol* **149:** 697–706

Boal D (2002) *Mechanics of the Cell*. Cambridge: Cambridge University Press, pp 175–208

Cannon GJ, Swanson JA (1992) The macrophage capacity for phagocytosis. *J Cell Sci* **101:** 907–913

Caron E, Hall A (1998) Identification of two distinct mechanisms of phagocytosis controlled by different Rho GTPases. *Science* **282:** 1717–1721

Champion JA, Mitragotri S (2006) Role of target geometry in phagocytosis. *Proc Natl Acad Sci USA* **103:** 4930–4934

Cougoule C, Hoshino S, Dart A, Lim J, Caron E (2006) Dissociation of recruitment and activation of the small G-protein Rac during Fc gamma receptor-mediated phagocytosis. *J Biol Chem* **281:** 8756–8764

Cougoule C, Wiedemann A, Lim J, Caron E (2004) Phagocytosis, an alternative model system for the study of cell adhesion. *Semin Cell Dev Biol* **15:** 679–689

Ezekowitz RA, Williams DJ, Koziel H, Armstrong MY, Warner A, Richards FF, Rose RM (1991) Uptake of Pneumocystis carinii mediated by the macrophage mannose receptor. *Nature* **351:** 155–158

Gao H, Shi W, Freund LB (2005) Mechanics of receptor-mediated endocytosis. *Proc Natl Acad Sci USA* **102:** 9469–9474

Garin J, Diez R, Kieffer S, Dermine JF, Duclos S, Gagnon E, Sadoul R, Rondeau C, Desjardins M (2001) The phagosome proteome: insight into phagosome functions. *J Cell Biol* **152:** 165–180

Gessner JE, Heiken H, Tamm A, Schmidt RE (1998) The IgG Fc receptor family. *Ann Hematol* **76:** 231–248

Greenberg S, Burridge K, Silverstein SC (1990) Colocalization of F-actin and talin during Fc receptor-mediated phagocytosis in mouse macrophages. *J Exp Med* **172:** 1853–1856

Griffin Jr FM, Silverstein SC (1974) Segmental response of the macrophage plasma membrane to a phagocytic stimulus. *J Exp Med* **139:** 323–336

Griffin Jr FM, Griffin JA, Leider JE, Silverstein SC (1976) Studies on the mechanism of phagocytosis. I. Requirements for circumferential attachment of particle-bound ligands to specific receptors on the macrophage plasma membrane. *J Exp Med* **142:** 1263–1282

Grinnell F, Geiger B (1986) Interaction of fibronectin-coated beads with attached and spread fibroblasts. Binding, phagocytosis, and cytoskeletal reorganization. *Exp Cell Res* **162:** 449–461

Groves E, Dart AE, Covarelli V, Caron E (2008) Molecular mechanisms of phagocytic uptake in mammalian cells. *Cell Mol Life Sci* **65:** 1957–1976

Hackam DJ, Rotstein OD, Sjolin C, Schreiber AD, Trimble WS, Grinstein S (1998) v-SNARE-dependent secretion is required for phagocytosis. *Proc Natl Acad Sci USA* **95:** 11691–11696

Henry RM, Hoppe AD, Joshi N, Swanson JA (2004) The uniformity of phagosome maturation in macrophages. *J Cell Biol* **164:** 185–194

Herant M, Heinrich V, Dembo M (2005) Mechanics of neutrophil phagocytosis: behavior of the cortical tension. *J Cell Sci* **118:** 1789–1797

Herant M, Heinrich V, Dembo M (2006) Mechanics of neutrophil phagocytosis: experiments and quantitative models. *J Cell Sci* **119:** 1903–1913

Lowry MB, Duchemin AM, Robinson JM, Anderson CL (1998) Functional separation of pseudopod extension and particle internalization during Fc gamma receptor-mediated phagocytosis. *J Exp Med* **187:** 161–176

Mitchell MA, Huang MM, Chien P, Indik ZK, Pan XQ, Schreiber AD (1994) Substitutions and deletions in the cytoplasmic domain of the phagocytic receptor Fc gamma RIIA: effect on receptor tyrosine phosphorylation and phagocytosis. *Blood* **84:** 1753–1759

Morrissette NS, Gold ES, Guo J, Hamerman JA, Ozinsky A, Bedian V, Aderem AA (1999) Isolation and characterization of monoclonal antibodies directed against novel components of macrophage phagosomes. *J Cell Sci* **112:** 4705–4713

Niedergang F, Colucci-Guyon E, Dubois T, Raposo G, Chavrier P (2003) ADP ribosylation factor 6 is activated and controls membrane delivery during phagocytosis in macrophages. *J Cell Biol* **161:** 1143–1150

Odin JA, Edberg JC, Painter CJ, Kimberly RP, Unkeless JC (1991) Regulation of phagocytosis and $Ca2^{+}$ flux by distinct regions of an Fc receptor. *Science* **254:** 1785–1788

Phillips DJ, Wells TW, Reimer CB (1987) Estimation of association constants of 42 monoclonal antibodies to human IgG epitopes using a fluorescent sequential-saturation assay. *Immunol Lett* **17:** 159–168

Stuart LM, Boulais J, Charriere GM, Hennessy EJ, Brunet S, Jutras I, Goyette G, Rondeau C, Letarte S, Huang H, Ye P, Morales F, Kocks C, Bader JS, Desjardins M, Ezekowitz RA (2007) A systems biology analysis of the *Drosophila* phagosome. *Nature* **445:** 95–101

Stuart LM, Ezekowitz RA (2008) Phagocytosis and comparative innate immunity: learning on the fly. *Nat Rev Immunol* **8:** 131–141

Swanson JA (2008) Shaping cups into phagosomes and macropinosomes. *Nat Rev Mol Cell Biol* **9:** 639–649

Swanson JA, Hoppe AD (2004) The coordination of signaling during Fc receptor-mediated phagocytosis. *J Leukoc Biol* **76:** 1093–1103

Touret N, Paroutis P, Terebiznik M, Harrison RE, Trombetta S, Pypaert M, Chow A, Jiang A, Shaw J, Yip C, Moore HP, van der Wel N, Houben D, Peters PJ, de Chastellier C, Mellman I, Grinstein S (2005) Quantitative and dynamic assessment of the contribution of the er to phagosome formation. *Cell* **123:** 157–170

Zhelev DV, Needham D, Hochmuth RM (1994) Role of the membrane cortex in neutrophil deformation in small pipets. *Biophys J* **67:** 696–705

Zigmond SH, Hirsch JG (1972) Effects of cytochalasin B on polymorphonuclear leucocyte locomotion, phagocytosis and glycolysis. *Exp Cell Res* **73:** 383–393